Original Study

Development and first clinical use of a novel anatomical and biomechanical testing platform for scoliosis

Michael A. Bohl, Sarah McBryan, Peter Nakaji, Steve W. Chang, Jay D. Turner, U. Kumar Kakarla

Department of Neurosurgery, Barrow Neurological Institute, St. Joseph's Hospital and Medical Center, Phoenix, AZ, USA

Contributions: (I) Conception and design: MA Bohl, S McBryan, UK Kakarla; (II) Administrative support: MA Bohl, S McBryan, P Nakaji; (III) Provision of study materials or patients: P Nakaji, SW Chang, JD Turner, UK Kakarla; (IV) Collection and assembly of data: MA Bohl, S McBryan; (V) Data analysis and interpretation: MA Bohl, S McBryan, SW Chang, JD Turner, UK Kakarla; (VI) Manuscript writing: All authors; (VII) Final approval of manuscript: All authors.

Correspondence to: U. Kumar Kakarla, MD. c/o Neuroscience Publications; Barrow Neurological Institute, St. Joseph's Hospital and Medical Center, 350 W. Thomas Rd.; Phoenix, AZ 85013, USA. Email: Neuropub@barrowneuro.org.

Background: Previous studies have demonstrated that, by using various three-dimensional (3D) printing technologies, synthetic spine models can be manufactured to mimic a human spine in its gross and radiographic anatomy and the biomechanical performance of bony and ligamentous tissue. These manufacturing processes have not, however, been used in combination to create a long-segment, biomimetic model of a patient with scoliosis. The purpose of this study was to describe the development of a biomimetic scoliosis model and early clinical experience using this model as a surgical planning and education platform.

Methods: Synthetic spine models were printed to mimic the anatomy and biomechanical performance of 2 adult patients with scoliosis. Preoperatively, the models were surgically corrected by the attending surgeon of each patient. Patients then underwent surgical correction of their spinal deformities. Correction of the models was compared to the surgical correction in the patients.

Results: Patient 1 had a preoperative coronal Cobb angle of 40° from L1 to S1, as did the patient's synthetic spine model. The patient's spine model was corrected to 17.6°, and the patient achieved a correction of 17.3°. Patient 2 had a preoperative mid-thoracic Cobb angle of 88° and an upper thoracic Cobb angle of 43°. Preoperatively, the patient's spine model was corrected to 19.5° and 9.2° for the mid-thoracic and upper thoracic curves, respectively. Immediately after surgery, the patient's mid-thoracic and upper thoracic Cobb angles measured 18.7° and 9.5°, respectively. In both cases, the use of the spine models preoperatively changed the attending surgeon's operative plan.

Conclusions: A novel synthetic spine model for corrective scoliosis procedures is presented, along with early clinical experience using this model as a surgical planning platform. This model has tremendous potential not only as a surgical planning platform but also as an adjunct to patient consent, surgical education, and biomechanical research.

Keywords: Three-dimensional printing (3D); adult spinal deformity; idiopathic scoliosis; surgical education

Introduction

Three-dimensional (3D) printing is an additive manufacturing process that has numerous potential applications in the field of spine surgery. These applications include the creation of custom pedicle screw guides, implants for complex spinal reconstructions, anatomical models for patient consent and surgical education, and scaffolds for laboratory regeneration of disc tissue (1-6). Some institutions now regularly request patient-specific 3D-printed models of patients undergoing complex spinal

reconstructions, as these models have demonstrated utility as an anatomical reference for patient education, preoperative planning, and intraoperative reference. However, a major drawback of these models is that their fidelity to a human spine is limited entirely to their gross anatomical appearance.

The increasing ability of 3D manufacturing technologies to mimic various human features portends the potential development of a synthetic spine model with both high anatomical and biomechanical fidelity (2-4,7-15). The potential utility of a customizable spine model with high biomechanical fidelity is tremendous, with potentially disruptive effects on fields such as spine biomechanics research, surgical education, surgical planning, and medical device testing. Spine biomechanics research, for example, is primarily limited by the use of cadaveric specimens (16-18). Although cadavers represent a gold standard model in terms of gross anatomy, their performance as a biomechanical platform is very limited by their high variability in tissue quality, limited shelf-life, high cost, and inability to model anything other than normal anatomy. A customizable synthetic spine model with high biomechanical fidelity would provide lower costs, lower variability between specimens (and therefore better data in comparison studies), and most importantly would enable the biomechanical testing of various pathologies in bone quality, spinal alignment, and spinal curvature (9). In the realm of surgical education, a high-fidelity model of scoliosis would enable trainees to practice certain corrective maneuvers they are otherwise unable to practice on cadaveric specimens (due to the difficulty in obtaining a cadaveric spine with scoliosis) (13). Demonstrating proficiency on such models might enable the quicker advancement of residents and fellows to higher levels of responsibility in the operating room and result in an overall faster learning curve toward becoming safe and independent spinal reconstruction surgeons (19). This model would also have potential utility as a surgical planning device, as it would enable surgeons to perform a given procedure on a patient-specific model before going to the operating room. Medical device manufacturers could use these models, rather than cadavers, to test new implants or instrument sets. The customizable nature of a synthetic 3D-printed model would be appealing in this realm as it would enable the testing of new equipment on a wide range of bone qualities and pathological anatomies.

Through a unique educational program in medical device innovation (20), residents at the authors' home institution attempted to create a novel 3D-printed and customizable spine model of scoliosis capable of mimicking a patient's gross anatomy, radiographic anatomy, biomechanical performance of pedicle screws, and soft-tissue performance on spinal range of motion testing. Previous studies from the authors' laboratory have shown that, by using various 3D printing technologies, synthetic models of the human spine can be manufactured in a way that enables them to mimic each of these features of the human spine in isolation (7-9). However, these manufacturing processes had not been used in combination to create a long-segment biomimetic spine model of a patient with scoliosis. This manuscript describes the development of this synthetic spine model and our early clinical experience using this model as a surgical planning platform.

Methods

Model manufacturing

A high-resolution computed tomogram of the thoracic and lumbar spines of 2 patients with scoliosis were uploaded into the Mimics InPrint software package (Materialise, NV, Leuven, Belgium), which was then used to threshold the vertebral bodies from T1 to the sacrum (*Figure 1*). The isolated vertebral bodies were then compiled into solid parts and transferred to the Autodesk Meshmixer software package (Autodesk, Inc., San Rafael, California, USA), where they were reassembled in the correct anatomical configuration and had intervertebral discs, anterior and posterior longitudinal ligaments, and facet capsules added. These models were then imported into the Simplify3D printing platform in segments of 3 to 5 disc levels to accommodate the size of the printing platform (Simplify3D, LLC, Blue Ash, Ohio, USA). Print parameters for the bone were chosen to mimic each patient's bone mineral density using a previously established curve correlating print settings to biomechanical performance of pedicle screws on insertional torque and axial pullout strength (7). Print parameters for the longitudinal ligaments, discs, and facet capsules were chosen based on data demonstrating analogous performance of certain materials and print settings to cadavers in range of motion testing, with subsequent changes in segmental range of motion dependent on disc space geometry (8). Each spine segment was then printed using a FlashForge Creator Pro (FlashForge Corp., Zhejiang, China) 3D printer with dual extruders. The spine segments were then reassembled and

Figure 1 Screenshot of spinal column of patient 1 after thresholding the vertebral bodies out of the computed tomogram and reconstructing the disc spaces into their correct anatomical location. Used with permission from Barrow Neurological Institute, Phoenix, Arizona.

the sacrum of each model was potted in a casting mold of Smooth-Cast 300Q resin (Smooth-On, Macungie, Pennsylvania, USA) for easier fixation of the model to an operating table.

Model testing

Each model was secured at the potted sacrum in a table vise with the mid-thoracic and upper thoracic spines supported by towels. Using a full kit of basic surgical instruments, including bone rongeurs, osteotomes, and a high-speed drill, as well as the same types of pedicle screws, rods, and reduction instruments planned for use in the operating room, the spine models were surgically corrected. Coronal Cobb angles of the spine models were measured before
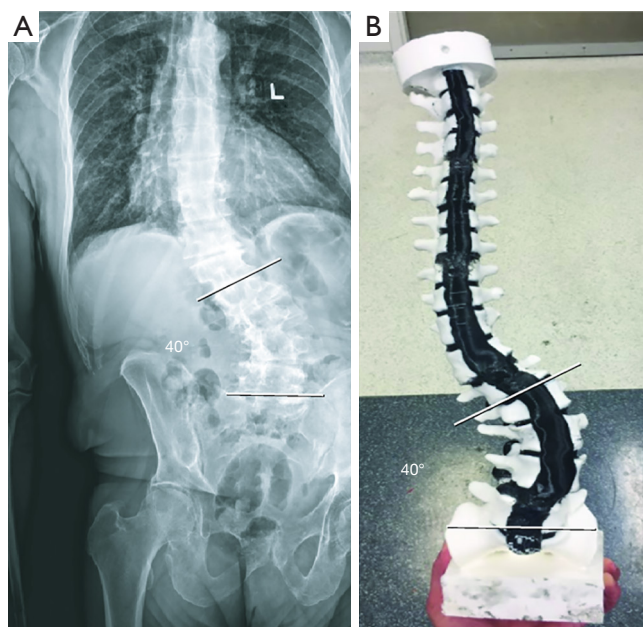
Figure 2 Patient 1. (A) Preoperative standing anteroposterior radiograph of patient 1 showing a 40° coronal Cobb angle measured from the L5–S1 disc space to the L1–L2 disc space, with the curve apex at L3, and (B) matching photograph of the anterior view of the 3D-printed spine model with identical Cobb angle. Used with permission from Barrow Neurological Institute, Phoenix, Arizona.

and after surgical correction. The attending surgeon for each patient was responsible for correcting the models in the laboratory prior to each case. This attending surgeon is fellowship trained in adult and pediatric spinal deformity and has 10 years of experience managing an academic spinal deformity practice.

Case 1

Patient 1 was a 70-year-old man with a history of multiple sclerosis and prior C2–T4 fixation and fusion who developed debilitating mid-lumbar and lower thoracic pain. He reported difficulty ambulating distances longer than 100 feet due to burning back pain, pressure, and lower extremity heaviness and was most comfortable sitting or lying flat in a recliner. Standing radiographs demonstrated a 40° left curve with apex at L3 (*Figure 2A*). High-resolution computed tomography demonstrated open facets and disc spaces without autofusion. A 3D model of the patient's spine was printed as previously described and used as an anatomical reference for obtaining patient consent for a

Figure 3 Video of the attending spine surgeon for patient 1 correcting the patient's scoliosis model preoperatively (21). Note how the model deforms at the disc spaces under the stress of the surgeon's in-situ bending of the rod (00:00–00:06). Used with permission from Barrow Neurological Institute, Phoenix, Arizona. Available online: http://www.asvide.com/watch/32943

T4-pelvis spinal reconstruction and fusion (*Figure 2B*). Prior to the patient's scheduled procedure, the spine model was surgically corrected. The spine model withstood significant corrective forces including rod de-rotation, rod reduction, and *in situ* bending without failure (*Figure 3*). When excessive reduction forces were placed on the pedicle screws, the screws began to pull out of the vertebral bodies as would be expected intraoperatively. During the surgical correction of the model, the attending surgeon discovered that he achieved a better result by placing the concave rod first to control the proximal end of the curve and beginning to reduce the curve before placing the convex rod and rotating this rod into the convex pedicle screws to achieve axial, coronal, and sagittal restoration. This surgical correction technique differed from the attending physician's routine plan to place the convex rod first and rotate this rod prior to placing the concave rod.

Case 2

Patient 2 was a 32-year-old woman with a history of adolescent idiopathic scoliosis who received a diagnosis at 9 years of age with an 18° mid-thoracic curve. She opted for bracing through adolescence and reached bone maturity with a mid-thoracic curve of 55°. After multiple pregnancies, she progressed to a Lenke class 2A morphology with a mid-thoracic curve of 88° and an upper thoracic curve of 43° (*Figure 4A*). She presented at age 32 complaining of debilitating mid-thoracic and upper
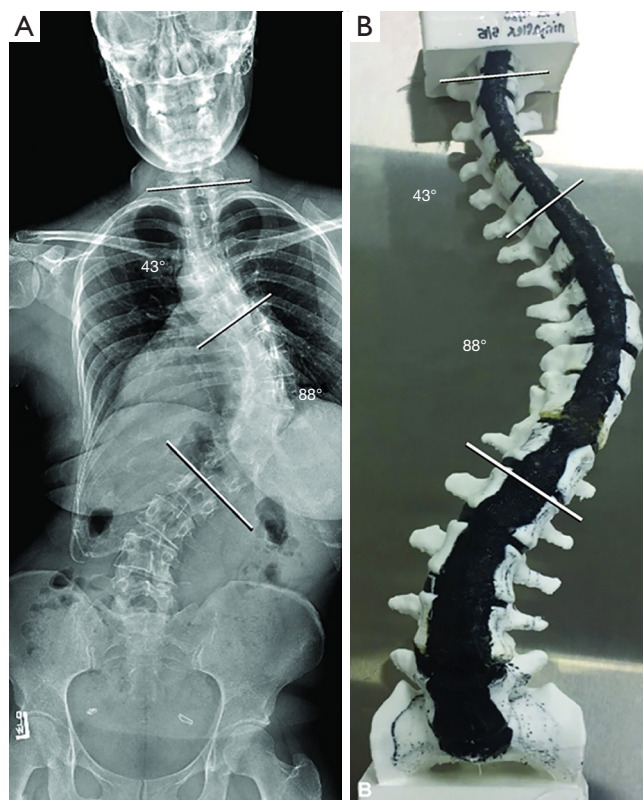
Figure 4 Patient 2. (A) Preoperative standing anteroposterior radiograph of patient 2 showing an 88° coronal Cobb angle measured at the main thoracic curve and 43° coronal Cobb angle at the upper thoracic curve, and (B) matching photograph of the anterior view of the 3D-printed spine model with identical 88° coronal Cobb angle measured at the main thoracic curve and 43° coronal Cobb angle at the upper thoracic curve. Used with permission from Barrow Neurological Institute, Phoenix, Arizona.

thoracic pain as well as episodes of breathing difficulty with physical exertion. A 3D-printed model of the patient's spine was made and was used as an anatomical reference for obtaining patient consent for a T2–L2 or L3 spinal reconstruction and fusion (*Figure 4B*). Before the patient's scheduled procedure, the spine model was surgically corrected by placing the concave rod first followed by the convex rod using differential contouring. During correction of the model, the attending surgeon decided that a lower instrumented level of L2 would provide adequate correction of the patient's main thoracic curve. In addition, many of the concave pedicles were difficult to cannulate due to their small size, and these levels were skipped during the actual surgical procedure on the basis of experience gained from
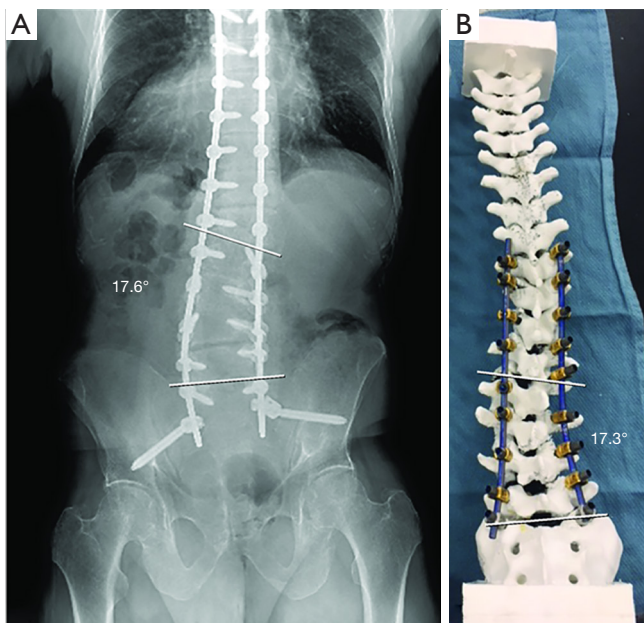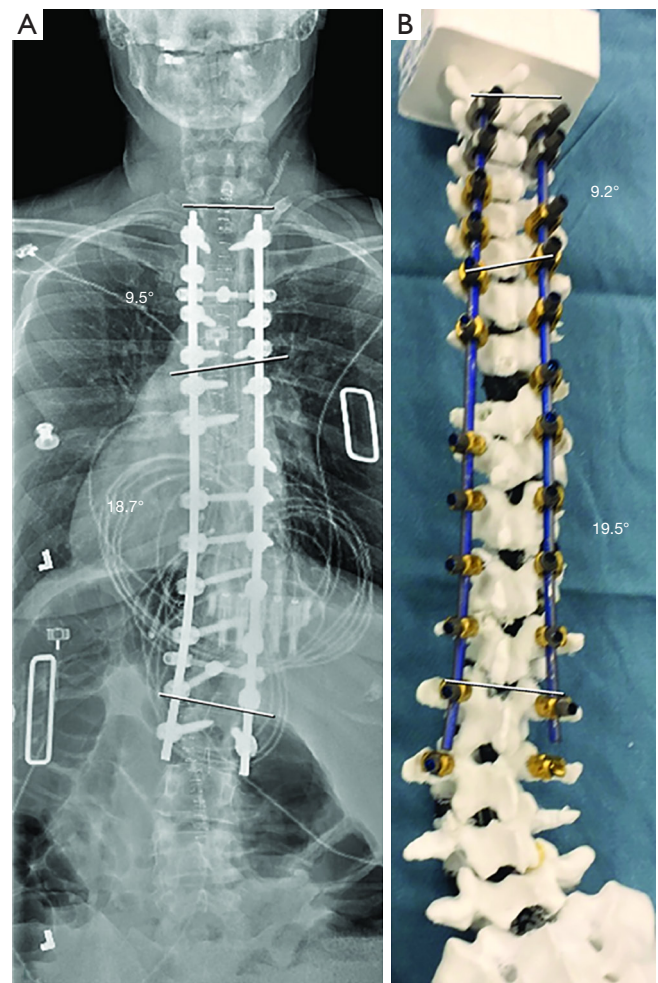
Figure 5 Patient 1. (A) Immediate postoperative standing posteroanterior radiograph of patient 1 showing a corrected coronal Cobb angle of 17.6°, and (B) matching photograph of the posterior view of the spine model showing a corrected coronal Cobb angle of 17.3°. Used with permission from Barrow Neurological Institute, Phoenix, Arizona.

correcting the spine model.

Results

Patient 1 had an uneventful operative course and was discharged from the hospital to an acute rehabilitation facility on postoperative day 8. At his 6-month follow-up visit, he reported a 90% improvement in his preoperative symptoms, and his standing radiographs demonstrated no hardware complication and maintenance of the surgical correction. A comparison of the patient's spinal alignment in postoperative radiographs to the spinal alignment of the model after surgical correction demonstrated close correlation, with a coronal Cobb angle of 17.6° and 17.3° for the patient and the model, respectively (*Figure 5A,B*).

Patient 2 had an uneventful operative course and was discharged from the hospital to home on postoperative day 7. At her 6-month follow-up visit, she reported an 80% improvement in her preoperative symptoms. She continued to undergo physical therapy as she had gained over 6 inches in height following her scoliosis correction and was taking some time to become accustomed to her new height. Six-

Figure 6 Patient 2. (A) Immediate postoperative standing posteroanterior radiograph of patient 2 showing a corrected main thoracic coronal Cobb angle of 18.7° and a corrected upper thoracic coronal Cobb angle of 9.5°, and (B) photograph of the posterior view of the spine model showing a corrected main thoracic coronal Cobb angle of 19.5° and an upper thoracic coronal Cobb angle of 9.2°. Used with permission from Barrow Neurological Institute, Phoenix, Arizona.

month standing radiographs demonstrated no hardware complication and maintenance of the surgical correction. A comparison of her spinal alignment in the postoperative radiographs to the spinal alignment of the model after surgical correction demonstrated close correlation, with a coronal Cobb angle for the main thoracic curve of 18.7° and 19.5° for the patient and model, respectively, and a coronal Cobb angle of the upper thoracic curve of 9.5° and 9.2° for the patient and model, respectively (*Figure 6*).

Discussion

The results of this study demonstrate the potential utility of the biomimetic spine model as a surgical planning platform for adult spinal reconstructions. Not only did the surgical correction of the models predict the extent of curve correction achieved intraoperatively but the attending surgeon changed his surgical plan after correcting each model preoperatively. Although it is difficult for us to know with certainty whether the models had an overall positive impact on these patients' surgical outcomes, one can safely presume that rehearsal of a complex procedure, especially a rehearsal that results in a changed surgical plan, is likely advantageous to surgical efficiency and safety.

The advent of 3D printing is generating a broad paradigm shift in surgical planning and education. Numerous studies have reported on the utility of 3D-printed models as surgical simulators in multiple fields including cranial neurosurgery, otorhinolaryngology, and cardiology (10,22-27). 3D-printed models are particularly fitting to the field of spine surgery, as training in this field requires hands-on work with specific pathological anatomies that are rarely, if ever, obtainable in a cadaver (e.g., various types of scoliosis, spondylosis, and spondylolisthesis). Furthermore, surgical education relies on the haptic feedback obtained from using surgical instruments on a realistic substrate, as this provides the dexterity training needed to safely and proficiently handle potentially dangerous instruments near sensitive neural structures. An increasing number of reports are being published in the spine surgery literature on various 3D-printed models that have demonstrated utility to surgical education and planning processes (5,11,12,28,29). The model described in this report is a logical next step for this technology as it takes customizable bony and soft-tissue components, each of which have demonstrated utility in isolation as high-fidelity models of their analogous human tissue, and combines them in a single long-segment model of complex anatomy. The resultant model has the potential to serve as a high-fidelity platform for biomechanics research, surgical planning, and resident and fellow education in scoliosis corrections.

Limitations and future directions

Further work is needed to validate the biomechanical performance of this model before it can be validated as a platform for biomechanical research. However, the early clinical results presented here are promising for the eventual validation of this technology as an adjunct, perhaps even replacement, for cadavers in spine biomechanical research. Efforts to generate the necessary data to begin this validation are currently underway.

The development of the presented scoliosis models has also been completed in parallel with an effort from the same laboratory to develop a short segment spine model with certain high-fidelity physiological functions such as bleeding bone, thecal sac, electrically conductive nerve roots, blood vessels, and surrounding radiolucent soft tissue. Early successes combining these features into a short segment model are an encouraging step toward the eventual development of a long-segment model of scoliosis that includes not only biofidelity to bony and ligamentous structures but also physiological feedback in terms of blood loss, spinal fluid leaks, and intraoperative neuromonitoring. Efforts to prototype this kind of comprehensive spine model are also underway.

Given the potential clinical benefit of having a high-fidelity spine model for surgical planning, it is important to discuss the potential costs of creating these models. The models used in this study were developed and manufactured in a prototyping laboratory at the authors' institution (20). The material cost alone of these models was less than $50. The commercial cost of these types of models would, however, be significantly higher, as the cost of printers, personnel, and other overhead would have to be taken into account. It is estimated that the commercial cost of these models would be between $300 and $800, depending on the number of spinal levels included and whether the model would include a pelvis, skull, and/or rib cage. Although this cost is not insignificant, it is amenable to a positive cost-benefit analysis if further studies demonstrate that use of the models leads to improved surgical planning, shorter operative times, and fewer postoperative complications. Future studies will be required to demonstrate whether this is in fact true.

Finally, this project arose from a novel resident education program in medical device education (20). As part of their education, residents work with patent law and engineering students at affiliated universities to prototype their ideas and write patent applications. During the peer-review process, the patent filing describing this new technology was licensed to a new company, thereby creating a potential conflict of interest that did not exist at the time of data collection, data analysis, or manuscript drafting and submission. This patent is owned and licensed by the hospital where this work took place. Because this potential conflict arose in the late stages

of peer review, we do not believe that it had any effect on our data collection, analysis, or reporting of results.

Conclusions

A novel anatomical and biomechanical model for corrective scoliosis procedures is presented, along with early clinical experience using this model as a surgical planning platform. In both cases, the preoperative correction of the synthetic spine model impacted the attending surgeons' surgical plan and accurately predicted the extent of curve correction achieved intraoperatively. This model has tremendous potential not only as a surgical planning platform, but also as an adjunct to surgical education and biomechanical research.

Acknowledgments

Footnote

Conflicts of Interest: MA Bohl is the inventor on a patent filing describing the technology evaluated in this study. The patent is owned by the institution where this work took place. This patent filing was licensed to a new company during the peer-review process. MA Bohl, S McBryan, and UK Kakarla have financial interests in the new company that licensed the patent. The other authors have no conflicts of interest to declare.

Ethical Statement: The authors are accountable for all aspects of the work in ensuring that questions related to the accuracy or integrity of any part of the work are appropriately investigated and resolved.

References

1. Choy WJ, Mobbs RJ, Wilcox B, et al. Reconstruction of thoracic spine using a personalized 3D-printed vertebral body in adolescent with T9 primary bone tumor. World Neurosurg 2017;105:1032.e13-7.
2. Tian X, Caldwell J, DeKorte D, et al. (261) The development of 3D printed spine training models for educational purposes. J Pain 2016;17:S41.
3. Phan K, Sgro A, Maharaj MM, et al. Application of a 3D custom printed patient specific spinal implant for C1/2 arthrodesis. J Spine Surg 2016;2:314-8.
4. Goel A, Jankharia B, Shah A, et al. Three-dimensional models: an emerging investigational revolution for craniovertebral junction surgery. J Neurosurg Spine 2016;25:740-4.
5. Liew Y, Beveridge E, Demetriades AK, et al. 3D printing of patient-specific anatomy: a tool to improve patient consent and enhance imaging interpretation by trainees. Br J Neurosurg 2015;29:712-4.
6. Rosenzweig DH, Carelli E, Steffen T, et al. 3D-printed ABS and PLA scaffolds for cartilage and nucleus pulposus tissue regeneration. Int J Mol Sci 2015;16:15118-35.
7. Bohl MA, Mooney MA, Repp GJ, et al. The Barrow Biomimetic Spine: fluoroscopic analysis of a synthetic spine model made of variable 3D-printed materials and print parameters. Spine (Phila Pa 1976) 2018;43:E1368-75.
8. Bohl MA, Mooney MA, Repp GJ, et al. The Barrow Biomimetic Spine: comparative testing of a 3D-printed L4-L5 Schwab grade 2 osteotomy model to a cadaveric model. Cureus 2018;10:e2491.
9. Bohl MA, Morgan CD, Mooney MA, et al. Biomechanical testing of a 3D-printed L5 vertebral body model. Cureus 2019;11:e3893.
10. Bagaria V, Chaudhary K. A paradigm shift in surgical planning and simulation using 3Dgraphy: experience of first 50 surgeries done using 3D-printed biomodels. Injury 2017;48:2501-8.
11. Park HJ, Wang C, Choi KH, et al. Use of a life-size three-dimensional-printed spine model for pedicle screw instrumentation training. J Orthop Surg Res 2018;13:86.
12. Wu AM, Shao ZX, Wang JS, et al. The accuracy of a method for printing three-dimensional spinal models. PLoS One 2015;10:e0124291.
13. Bohl MA, McBryan S, Spear C, et al. Evaluation of a novel surgical skills training course: are cadavers still the gold standard for surgical skills training? World Neurosurg 2019;127:63-71.
14. Bohl MA, Zhou JJ, Mooney MA, et al. The Barrow Biomimetic Spine: effect of a 3-dimensional-printed spinal osteotomy model on performance of spinal osteotomies by medical students and interns. J Spine Surg 2019;5:58-65.
15. Bohl MA, Mauria R, Zhou JJ, et al. The Barrow Biomimetic Spine: face, content, and construct validity of a 3D-printed spine model for freehand and minimally invasive pedicle screw insertion. Global Spine J 2019;9:635-41.
16. Tomlinson JE, Yiasemidou M, Watts AL, et al. Cadaveric

spinal surgery simulation: a comparison of cadaver types. Global Spine J 2016;6:357-61.

17. Gonzalez-Blohm SA, Doulgeris JJ, Lee WE 3rd, et al. The current testing protocols for biomechanical evaluation of lumbar spinal implants in laboratory setting: a review of the literature. Biomed Res Int 2015;2015:506181.

18. Newcomb A, Lehrman JN, Crawford NR. Variations among human spine segments and their relationships to in vitro kinematics: a retrospective analysis of 281 motion segments from 85 cadaveric spines. International Society for the Advancement of Spine Surgery 2017 (abstract 571); Boca Raton, FL.

19. Pavlidis I, Zavlin D, Khatri AR, et al. Absence of stressful conditions accelerates dexterous skill acquisition in surgery. Sci Rep 2019;9:1747.

20. Bohl MA, Mooney MA, Sheehy J, et al. The Barrow Innovation Center: a novel program in neurosurgery resident education and medical device innovation. Cureus 2018;10:e2142.

21. Bohl MA, McBryan S, Nakaji P, et al. Video of the attending spine surgeon for patient 1 correcting the patient's scoliosis model preoperatively. Asvide 2019;6:258. Available online: http://www.asvide.com/watch/32943

22. Bernardo A. Virtual reality and simulation in neurosurgical training. World Neurosurg 2017;106:1015-29.

23. Barber SR, Kozin ED, Dedmon M, et al. 3D-printed pediatric endoscopic ear surgery simulator for surgical training. Int J Pediatr Otorhinolaryngol 2016;90:113-8.

24. Del Castillo-Calcaneo J, Donoghue JA. A novel method for 3-dimensional printing a brain that feels and looks like one: the next step in the search of the perfect neurosurgical simulator. World Neurosurg 2016;91:620-2.

25. Cohen J, Reyes SA. Creation of a 3D printed temporal bone model from clinical CT data. Am J Otolaryngol 2015;36:619-24.

26. Olivieri LJ, Su L, Hynes CF, et al. "Just-in-time" simulation training using 3-D printed cardiac models after congenital cardiac surgery. World J Pediatr Congenit Heart Surg 2016;7:164-8.

27. Ryan JR, Almefty KK, Nakaji P, et al. Cerebral aneurysm clipping surgery simulation using patient-specific 3D printing and silicone casting. World Neurosurg 2016;88:175-81.

28. Cho W, Job AV, Chen J, et al. A review of current clinical applications of three-dimensional printing in spine surgery. Asian Spine J 2018;12:171-7.

29. Cramer J, Quigley E, Hutchins T, et al. Educational material for 3D visualization of spine procedures: methods for creation and dissemination. J Digit Imaging 2017;30:296-300.